

Ammonia Capture in Porous Organic Polymers Densely Functionalized with Brønsted Acid Groups

Jeffrey F. Van Humbeck,[†] Thomas M. McDonald,[†] Xiaofei Jing,[§] Brian M. Wiers,[†] Guangshan Zhu,[§] and Jeffrey R. Long^{*,†,‡}

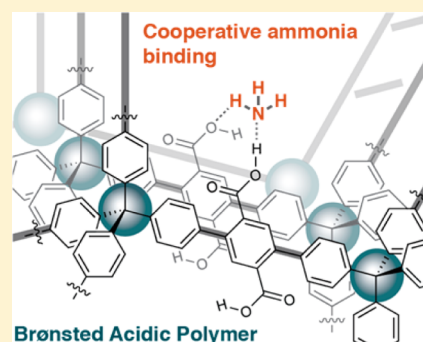
[†]Department of Chemistry, University of California, Berkeley, California 94720, United States

[‡]Material Science Division, Lawrence Berkeley National Laboratory, Berkeley, California, 94720, United States

[§]State Key Laboratory of Inorganic Synthesis and Preparative Chemistry, Jilin University, Changchun, China 130012

Supporting Information

ABSTRACT: The elimination of specific environmental and industrial contaminants, which are hazardous at only part per million to part per billion concentrations, poses a significant technological challenge. Adsorptive materials designed for such processes must be engendered with an exceptionally high enthalpy of adsorption for the analyte of interest. Rather than relying on a single strong interaction, the use of multiple chemical interactions is an emerging strategy for achieving this requisite physical parameter. Herein, we describe an efficient, catalytic synthesis of diamondoid porous organic polymers densely functionalized with carboxylic acids. Physical parameters such as pore size distribution, application of these materials to low-pressure ammonia adsorption, and comparison with analogous materials featuring functional groups of varying acidity are presented. In particular, BPP-5, which features a multiply interpenetrated structure dominated by <6 Å pores, is shown to exhibit an uptake of 17.7 mmol/g at 1 bar, the highest capacity yet demonstrated for a readily recyclable material. A complementary framework, BPP-7, features slightly larger pore sizes, and the resulting improvement in uptake kinetics allows for efficient adsorption at low pressure (3.15 mmol/g at 480 ppm). Overall, the data strongly suggest that the spatial arrangement of acidic sites allows for cooperative behavior, which leads to enhanced NH₃ adsorption.



1. INTRODUCTION

The adsorption of contaminants that are present in vanishingly low concentration—parts per million or below—presents a significant technical challenge in both environmental and industrial settings. To achieve meaningful adsorption capacity, an extremely high enthalpy of adsorption (ΔH_{ads}) is required. This energetic requirement typically lies well outside the range of physical adsorption processes and will instead require the development of materials that interact chemically with the analyte of interest.¹ Noteworthy progress has been achieved in the selective adsorption of 390–400 ppm carbon dioxide, as a first step toward its direct capture from air,^{2–4} and presents an interesting conceptual approach.^{5–8} Appropriate adsorption enthalpies are achieved in these cases through multiple chemical interactions: Initial interaction of a basic amine with the electrophilic carbon of CO₂ yields a carbamic acid, which is further stabilized through either full proton transfer to yield an ammonium carbamate ion pair⁹ or through hydrogen-bonding interactions (Figure 1a).¹⁰ A similar approach can be envisioned, whereby multiple acidic sites located in close proximity result in the strong adsorption of Lewis basic pollutants (Figure 1b).

Basic gases, such as ammonia, can lead to significant environmental and industrial concerns at similarly small

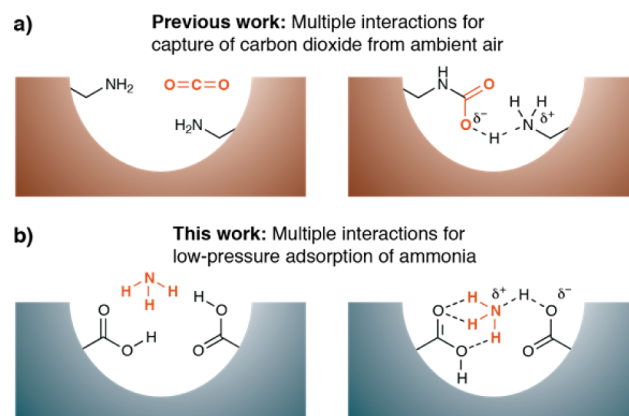


Figure 1. Strategy for the development of low-pressure ammonia adsorbents. (a) Multiple interactions for adsorption of low-pressure carbon dioxide. (b) Proposed approach to ammonia adsorption.

concentrations. With regards to human health, ammonia itself has a recommended CAL-OSHA permissible exposure limit of only 25 ppm, which can be encountered in numerous industrial

Received: October 14, 2013

Published: January 23, 2014

settings.¹¹ Highly toxic amines have even more stringent safety limits (e.g., diethanolamine, 0.46 ppm). In perhaps the most extreme example, volatile organic amines can disrupt photolithography at only tens of parts per billion concentration, resulting in characteristic ‘T-top’ channel features that render the resulting silicon wafer useless (Figure 2a).^{12,13} As integrated


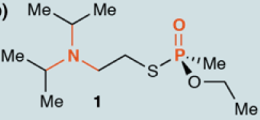
		REQUIRED MATERIAL STABILITY	
		Moderate	Very High
CAPTURE/STORAGE PRESSURE	High pressure		(c) NO_x NH_3 $\xrightarrow{\text{CSR}}$ N_2 H_2O On-board vehicle storage for Catalytic Selective Reduction
	Low pressure	(a)  >50 ppb NH_3 ‘T-top’ deformities in photolithography	(b)  1 Conserved basic residues in V-series nerve agents

Figure 2. Target applications for ammonia capture and storage based on ammonia/amine pressure and adsorbent stability requirements. (a) Air purification for semiconductor manufacture. (b) Ammonia as a first model for chemical warfare agents. (c) Use of ammonia as an on-board reducing agent to mitigate vehicle emissions.

circuits with narrower feature sizes are pursued, air purity requirements will become even more stringent,¹⁴ though these separation challenges are tempered by the fact that the low ammonia concentration will present only moderate demands on material stability. Outside of this specific application, low-pressure ammonia adsorption can also serve as the first model for a generic acid–base interaction, taking the place of important but difficult to handle analytes such as the V-series of nerve agents (e.g., VX 1, Figure 2b). At higher pressures, safe and reversible on-board storage for vehicle applications could be an enabling technology for ammonia-based fuel cells¹⁵ or more likely as a reducing agent for the mitigation of nitrogen oxide emissions (Figure 2c).^{16,17} Exposure to high ammonia pressures and the need for hundreds-to-thousands of adsorption cycles will present an exceptional demand on material stability, as will the diversity of potential environments where chemical weapons could be encountered.

Over the past 15 years, metal–organic frameworks (MOFs) have demonstrated their utility in numerous applications, including gas storage, molecular separations, sensing, and size-selective catalysis.^{18–24} Some preliminary investigations into the use of these materials for ammonia adsorption have also been conducted. The overwhelming majority of these examples use Lewis acidic framework sites to increase the strength of adsorption for NH_3 . In materials such as MOF-74, exposed metal cations provide the desired adsorption sites.²⁵ In related materials known as covalent organic frameworks (COFs), it has been demonstrated that three-coordinate boron centers can behave in a similar Lewis acidic fashion, with the framework generated from hexahydroxytriphenylene and biphenyldiboronic acid (COF-10) displaying high uptake at moderate pressure.²⁶

In the context of MOFs, the use of Brønsted acidic centers for the adsorption of ammonia has been explored to a much

lesser degree. Trikalitis reported a MOF-205²⁷ analog containing free phenolic –OH groups, which demonstrated excellent low- and moderate-pressure ammonia capacity.²⁸ However, the basic zinc acetate-type structure was not stable to ammonia exposure, with framework collapse suggested by powder X-ray diffraction and gas adsorption experiments, in line with previous observation made on analogous zinc-based materials (MOF-5 and MOF-177).^{29,30} In an effort to generate ammonia adsorbents that would be stable, and therefore potentially reusable, Yaghi investigated a zirconium-based UiO-66 analog³¹ featuring anilinium cations as the Brønsted acid source.³² Although only one-third of the available aniline sites in the material had been protonated, a meaningful increase in NH_3 adsorption was noted, and the framework survived exposure up to 1 bar of pressure.

Recently, porous organic polymers featuring a diamondoid-type structure have been introduced as ‘element–organic frameworks’ (e.g., EOF-1),³³ ‘porous aromatic frameworks’ (e.g., PAF-1),³⁴ and ‘poly(aryleneethynylene) networks’ (e.g., PAE-E1),³⁵ with initial investigations on ammonia capture using isolated metal catechol³⁶ and polyimide³⁷ functional groups reported. Two particular features of these materials, and PAF-1 in particular, suggested that they would be an excellent platform for the development of stable low-pressure ammonia adsorbents utilizing cooperative interactions. In addition to the high specific surface area of PAF-1, the physicochemical stability of this material is especially noteworthy. It exhibits pH stability ranging from anhydrous chlorosulfonic acid³⁸ to KOH/DMSO ‘superbase’³⁹ (*vide infra*). Not only does this suggest that exposure to ammonia will be easily tolerated, it also allows for a diverse range of postsynthetic chemical transformations. Already chloromethylation,⁷ nitration,⁴⁰ and sulfonation,³⁸ which occur under vigorously acidic conditions, have been demonstrated. We surmised that common Brønsted acidic functional groups (e.g., –CO₂H) that are difficult to include in MOFs, due to their metal complexation abilities, could be included into these networks, in a density that would be otherwise difficult to achieve.

Herein, we give a full account of the conceptual and experimental development that led from Brønsted acidic MOFs with single-point ammonia binding sites, to new porous organic polymers that display excellent low-pressure ammonia adsorption, with multiple functional groups present in a spatial arrangement that leads to cooperative reactivity.

2. EXPERIMENTAL SECTION

General experimental information, specific synthetic procedures, and full characterization for all new small molecules and organic polymers are available in the Supporting Information.

Generic Procedure for Bis(cyclooctadiene)nickel(0) Polymerization. The procedure applied was that reported for the original synthesis of PAF-1.³⁴ Bis(cyclooctadiene)nickel(0) (5.2 equiv was charged in an oven-dried Schlenk flask inside an inert atmosphere glovebox. The flask was sealed, removed, and connected to a standard manifold for further manipulation. Vacuum-dried 2,2’-bipyridine (5.2 equiv) was added against positive nitrogen pressure, followed by 1,5-cyclooctadiene (6.6 equiv) and anhydrous DMF (0.05 M concentration, relative to C–Br bonds). The solution was heated to 80 °C for 1 h. [Important note: At this point, the solution should be a vibrant, dark violet color, without any hint of black or brown. Occasionally, especially when older sources of DMF were used, a significant dulling of the purple color of the reagent was noted, and these reactions universally gave unsatisfactory results. This issue was never encountered when using freshly obtained anhydrous DMF of high commercial grade or DMF that had been stored under rigorously

anhydrous conditions, protected from light and heat.] Solid tetrakis(aryl bromide) (1.0 equiv, 4.0 equiv C–Br functional groups) was added to the vibrant purple solution against positive nitrogen pressure. The reaction was left to stir at 80 °C for 72 h. At that point, it was allowed to cool to room temperature, concentrated hydrochloric acid was added (one-half the volume of DMF), and the suspension was left to stir overnight. The resulting solid was collected by filtration and washed with water (5 washes with HCl volume), absolute ethanol (5 washes with HCl volume), and THF (5 washes with HCl volume). It was further purified by Soxhlet extraction with THF (24 h) and dried under vacuum at the specified temperature to yield the desired polymer.

Generic Procedure for Palladium-Catalyzed Polymer Synthesis. An oven-dried round-bottomed flask, cooled under N₂, was charged with a bis(pinacolborane)aryl monomer (2.1 equiv), tetrakis(4-bromophenyl)methane (1.0 equiv), and chloro(2-dicyclohexylphosphino-2',6'-dimethoxy-1,1'-biphenyl)[2-(2'-amino-1,1'-biphenyl)]-palladium(II) (0.70–1.1 mol % relative to –Br functional groups) and was purged for 10 min with flowing nitrogen. Degassed THF (0.042 M relative to tetrabromide) and degassed aqueous potassium carbonate (2 M, 10% of THF volume) were added, and the solution was heated to 60 °C for 48–72 h. During the course of the polymerization, the reaction became an extremely viscous gel. The gel was cooled to room temperature and was transferred onto a Büchner funnel with the aid of additional THF. With constant vacuum applied, the gel eventually collapsed into a free-flowing powder, which was washed with hot hydrochloric acid (3 N, 5 washes with triple THF volume), hot water (5 washes with triple THF volume), hot ethanol (5 washes with triple THF volume), and hot CHCl₃ (5 washes with triple THF volume). The resulting powder was then further purified by Soxhlet extraction with THF (24 h). The polymer was activated at the appropriate temperature under vacuum to deliver the desired material.

Generic Procedure for Side-Chain Cleavage to Yield Free Terephthalic Acid Polymers. A solid terephthalic ester polymer was charged, under N₂, in an oven-dried round-bottomed flask. Solid potassium hydroxide was added (135 wt %), followed by anhydrous DMSO (to 0.4 M KOH). The flask was heated to 150 °C for 24 h. After cooling to room temperature, the solid was collected by filtration, washed with methanol (3 washes with DMSO volume), and allowed to air dry on the Büchner funnel over vacuum for 15 min. The resulting solid was resubjected to identical basic conditions for another 24 h using fresh KOH/DMSO. This cycle was repeated a total of two to three times, depending on the substrate. After filtering and washing with methanol the final time, the resulting solid was suspended in hydrochloric acid (1 N, 50% of DMSO volume) at room temperature for 8 h. The acid was removed with a syringe, with care not to remove any polymer. Next, the solid was exposed to hydrochloric acid of higher concentration (3 N, 50% of DMSO volume) at room temperature for ~12 h. Again, the acid was removed by syringe, and water was added (50% of DMSO volume). The vial was left to sit at 80 °C for 1 h, at which point the water was removed by syringe and replaced with fresh water (50% of DMSO volume). This exchange was repeated twice more, before the polymer was finally collected by filtration. Soxhlet extraction with THF (16 h) delivered the final product, which was activated at the appropriate temperature under vacuum to deliver the desired porous acidic polymer.

3. RESULTS AND DISCUSSION

Brønsted Acidic MOFs. As reported previously, inclusion of hydrochloric acid equivalents in the 2-aminoterephthalic acid derivative of UiO-66 ([Zr₆O₄(OH)₄][p-(CO₂)₂C₆H₃NH₂]₆) allows for a significant increase in ammonia uptake, even with only one-third of the organic linkers protonated.³² In our hands, exposure of the neutral parent framework UiO-66-NH₂ to anhydrous hydrochloric acid in 1,4-dioxane did not result in any loss of crystallinity, although analysis of powder X-ray diffraction data could not unequivocally locate the chloride counterion in the presumed anilinium chloride UiO-66-NH₃Cl.

The ideal structure would deliver a moderate density (3.35 mmol/g) of anilinium sites, along with the weakly acidic hydroxide protons found in the inorganic cluster (2.23 mmol/g). For a representative example of a stronger Brønsted acid, Fe-MIL-101-SO₃H⁴¹ provides a comparable number of total acidic sites to UiO-66-NH₃Cl, distributed between the protic sulfonic acids (2.19 mmol/g) and Lewis acidic unsaturated metal centers (3.28 mmol/g). The room temperature (298 K) ammonia uptakes for these materials are shown in Figure 3.

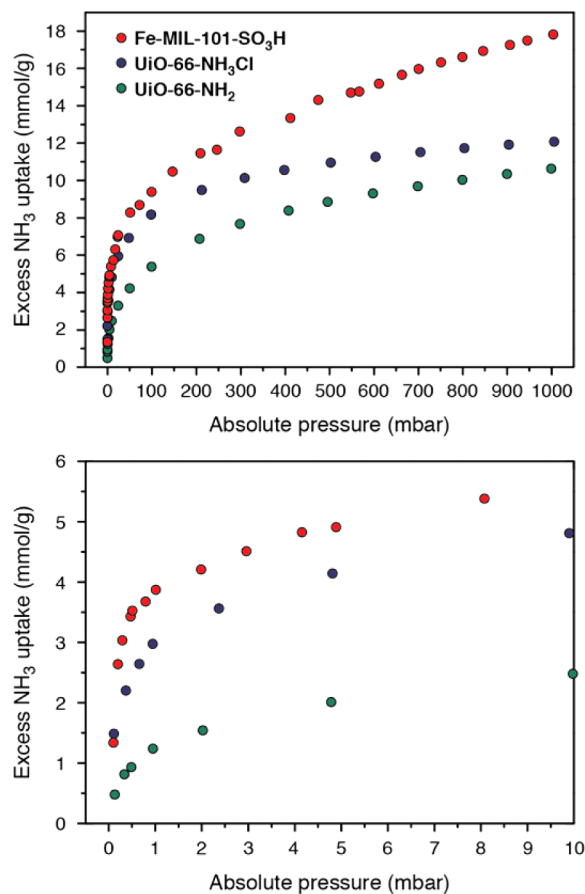


Figure 3. Ammonia adsorption at 298 K in Brønsted acidic MOFs (Fe-MIL-101-SO₃H: red circles, UiO-NH₃Cl: blue circles) and a nonacidic structure (UiO-66-NH₂: green circles).

The improvement in uptake, especially at low pressure, shown by UiO-66-NH₃Cl as compared to the parent framework (i.e., 0.93 mmol/g at 488 ppm for UiO-66-NH₂ vs 2.64 mmol/g at 663 ppm for UiO-66-NH₃Cl) confirms our prediction that Brønsted acidic adsorption sites could lead to meaningful ammonia adsorption at low pressure. Gratifyingly, the more acidic framework Fe-MIL-101-SO₃H yielded an exceptional adsorbent, which displayed improved uptake at low pressure (3.52 mmol/g at 510 ppm) and, owing to its significantly higher specific surface area, at higher pressure as well (17.80 mmol/g at 1004 mbar).

Porous Organic Polymers with Isolated Brønsted Acidic Substituents. Although encouraging performance was seen for low-pressure ammonia adsorption in UiO-66-NH₃Cl and Fe-MIL-101-SO₃H, these materials face certain practical limitations. Although UiO-66-NH₃Cl maintained crystallinity after controlled HCl addition, ammonia adsorption in this specific case results in the formation of NH₄Cl, which

prevents the reactivation and recycling of this material by a simple temperature and/or vacuum swing. Fe-MIL-101-SO₃H seemed like a more promising material for further optimization, with one significant caveat: with the appended sulfonic acids already delivering very high Brønsted acidity, it is not clear how the performance of this material could be improved further.

With high specific surface area and exceptional chemical stability, PAF-1 seemed like an ideal platform for the development of acidic adsorbents, especially those that must function for extended periods of time in high-pressure ammonia environments. Already, Zhou has described the conversion of PAF-1 into the analogous sulfonic acid-functionalized material (i.e., PPN-6-SO₃H: [(C₆H₄-C₆H₃SO₃H)₂(C)]),³⁸ and while we recognized that frameworks substituted with anilinium chloride groups (i.e., -NH₃Cl) would represent a suboptimal material due to NH₄Cl formation, it would allow for the effect of the framework backbone, as opposed to the functional group complement, to be directly interrogated. Our approach to the synthesis of the required materials is shown in Figure 4. The parent material

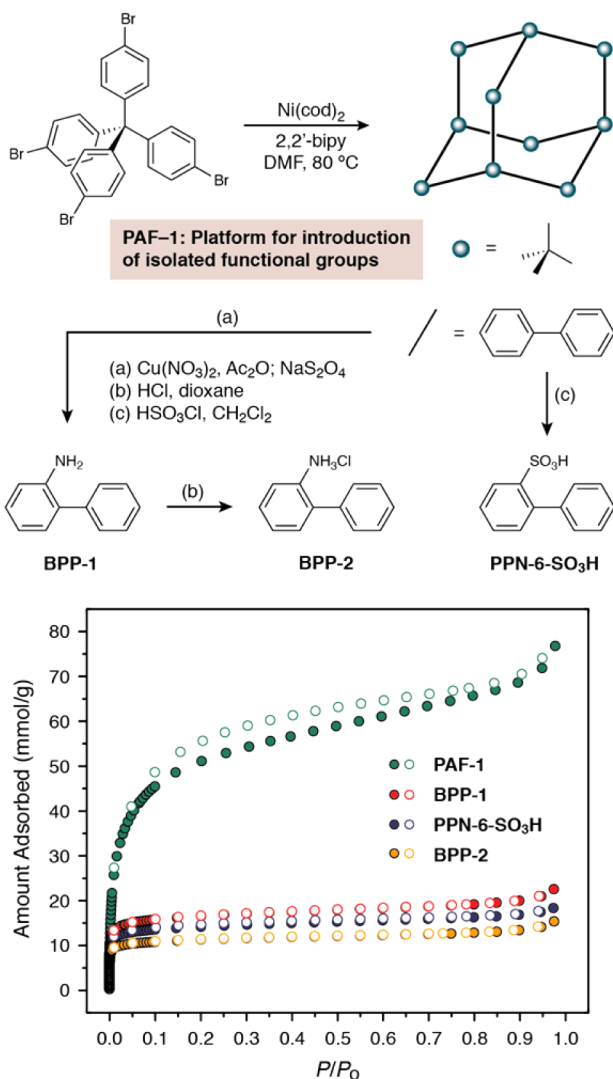


Figure 4. Synthesis and 77 K nitrogen adsorption characteristics of PAF-1 (green circles) and functionalized derivatives: BPP-1 (red circles), BPP-2 (yellow circles), and PPN-6-SO₃H (blue circles). Open circles represent desorption data.

(i.e., PAF-1) was synthesized according to the original procedure.³⁴ Menke conditions⁴²—a far milder alternative to HNO₃—introduce nitrogen as an aromatic nitro group, which was fully reduced to the corresponding aniline by sodium dithionite to deliver [(C₆H₄-C₆H₃NH₂)₂(C)] (BPP-1: Berkeley porous polymer-1), as indicated by FTIR analysis (see Supporting Information). Simple protonation with anhydrous hydrochloric acid provided the anilinium chloride-functionalized material [(C₆H₄-C₆H₃NH₃Cl)₂(C)] (BPP-2). Following the reported procedure,³⁸ exposure to chlorosulfonic acid affords the arylsulfonic acid polymer PPN-6-SO₃H. The nitrogen adsorption characteristics of these materials are also presented in Figure 4. Functional group addition to PAF-1 results in a significant reduction in the BET surface area, from 4240 m²/g in the parent framework to 1400 m²/g in BPP-1, 965 m²/g in BPP-2, and 1200 m²/g in PPN-6-SO₃H.

As expected, surface area as determined by N₂ adsorption is not predictive of ammonia uptake (Figure 5). Instead, there is a

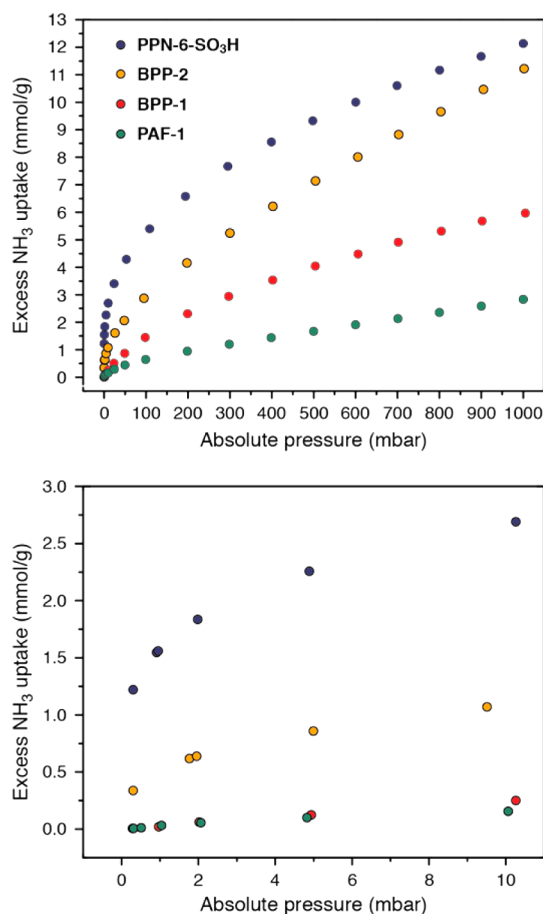


Figure 5. Room temperature (298 K) ammonia adsorption for PAF-1 (green circles), BPP-1 (red circles), BPP-2 (yellow circles), and PPN-6-SO₃H (blue circles).

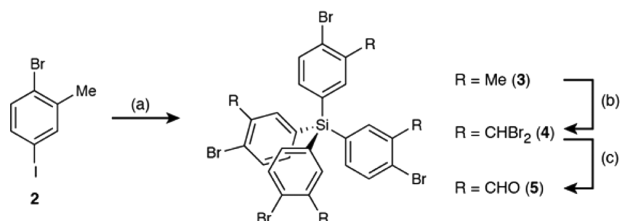
clear relationship between functional group acidity and adsorption, at both our low-pressure value of interest (500 ppm) and at the highest pressure investigated (1 bar). With relative acidity seemingly dominating adsorption performance, it is unsurprising that the MOFs investigated show better uptake for the same functional group substitutions (i.e., 2.64 mmol/g at 663 ppm for UiO-66-NH₃Cl vs 0.97 mmol/g at 636 ppm for BPP-2; 3.52 mmol/g at 510 ppm for Fe-MIL-101-

SO₃H vs 1.54 mmol/g at 919 ppm for PPN-6-SO₃H). The electron-withdrawing ability of the two carboxylate groups in the terephthalate linkers of the UiO-66 and MIL-101 series should increase the acidity of the ammonium chloride and sulfonic acid, respectively.

Porous Organic Polymers with Cooperative Brønsted Acidic Substituents. Given the ammonia uptake results obtained for MOFs and porous aromatic frameworks with isolated Brønsted acidic functional groups, it seemed likely that we would not be able to increase uptake substantially, especially at low pressure, through further tuning of the functional group, as sulfonic acids represented some of the most acidic groups that are readily accessible synthetically. Traditional adsorbents such as zeolites and activated carbons, which have been investigated in the context of ammonia adsorption, are similarly limited in their chemical tunability.^{30,43–46} Instead, we were inspired by recent computational results suggesting that the cooperative activity of multiple groups could have a strong positive effect on low-pressure adsorption.⁴⁷ Although the materials derived from PAF-1 displayed lower uptake, we preferred to base further development around this platform for a simple reason: Binding sites that contained multiple acidic functional groups (e.g., –CO₂H) close enough in space to interact with a single ammonia molecule would likely also bind metal atoms strongly, potentially disrupting MOF synthesis.

The monomer required to produce a close analog to PAF-1 (and also to EOF-1), with functional groups poised to interact cooperatively, was successfully synthesized employing the method presented in Scheme 1. Selective metalation of

Scheme 1. Synthesis of *meta*-Substituted Porous Organic Polymer Precursors^a



^aConditions: (a) *n*-BuLi, THF, –78 °C, then SiCl₄, –78 °C, 72%. (b) Benzoyl peroxide, *N*-bromosuccinimide, CCl₄, reflux 62%. (c) Dimethyl sulfoxide/acetic acid/water (90/5/5 v/v), 105 °C, 66%.

bromoiodoarene **2** and 4-fold addition to silicon tetrachloride produced tetra-*meta*-methylated arylsilane **3**. Selective 8-fold bromination under radical conditions yields **4**. All attempts to monobrominate each benzylic position selectively resulted in a mixture of doubly-, singly-, and nonbrominated methyl groups. Hydrolysis in wet and slightly acidic DMSO provides tetrakis(3-formyl-4-bromophenyl)silane **5**, which has both the halide atoms requisite for polymerization and a versatile functional group handle for postsynthetic modification.

Polymerization of **5** proceeded as expected under identical conditions as used previously to yield [(2,2'-(C₆H₃CHO-C₆H₃CHO)₂(Si)] (BPP-3), which bears functional groups in the positions directly adjacent to the biphenyl bond, poised to interact cooperatively during gas adsorption (Figure 6). However, we were surprised to find a surface area approximately one-half of what would be expected, based on the functionalized PAF-1 derivatives presented above (570 m²/g BET vs 965–1400 m²/g). While inefficient polymerization

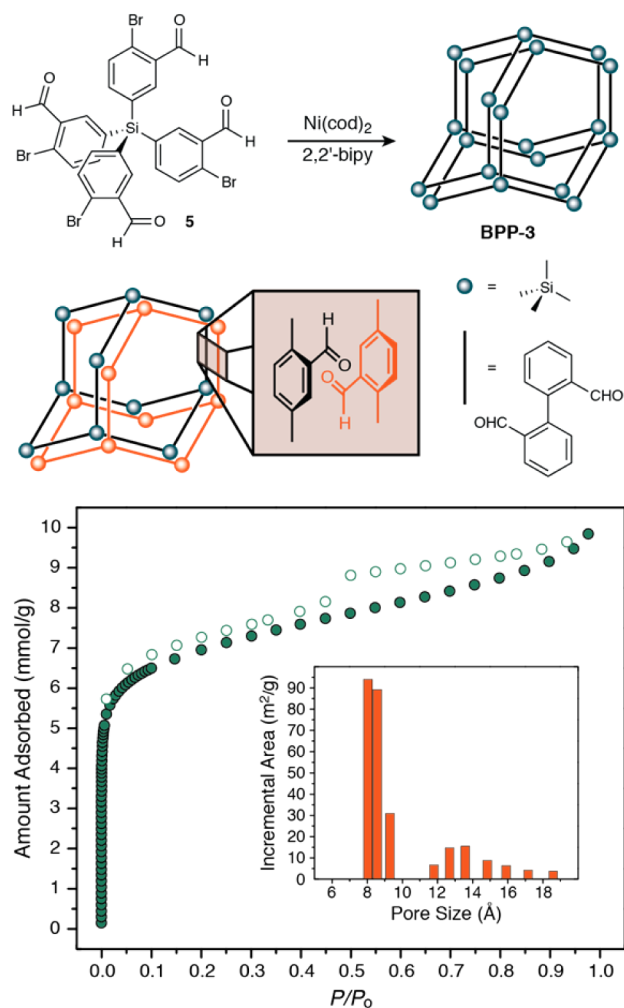


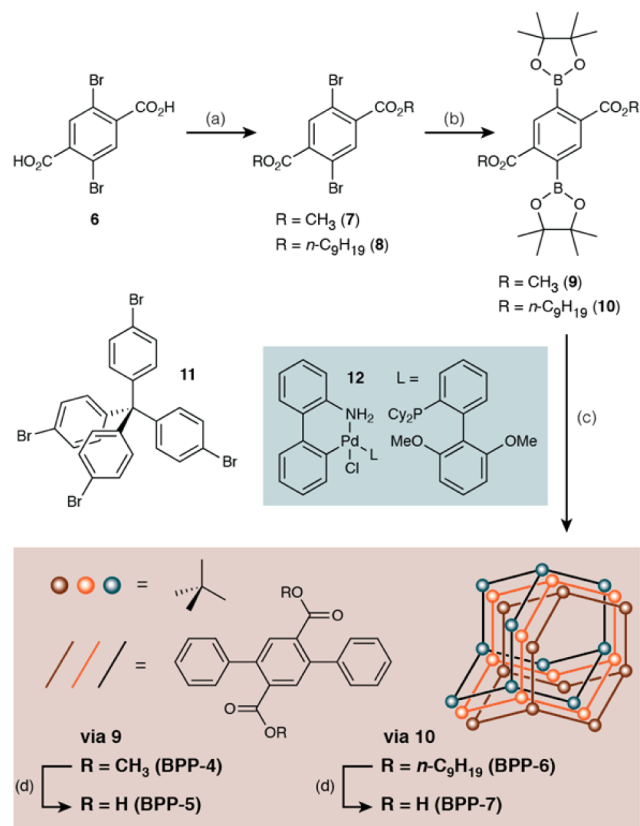
Figure 6. Polymerization, nitrogen adsorption characteristics (77 K), and pore size distribution for BPP-3. Open circles represent desorption data.

could explain such a low surface area, two important observations strongly suggest an alternative explanation. Analysis of residual bromine by energy dispersive X-ray spectroscopy (EDX) indicated no remaining bromine, to the limit of detection, suggesting that the low surface area observed was not due to a low degree of polymerization. Most importantly, pore size distribution revealed that the source of the low observed nitrogen uptake was framework interpenetration,^{48,49} with the dominant diameters being much smaller than the ~11 Å expected for an open-pore structure. As the steric parameters of functionalized monomer **5** are not remarkably different from the monomer used to synthesize PAF-1 (i.e., tetrakis(4-bromophenyl)methane), it seems likely that an increased attractive interaction between independent networks, due to the dipole–dipole interaction between the aldehyde substituents, drives interpenetration. Although network interpenetration results in lower specific surface area, it also offers a new design element that could potentially be leveraged for materials synthesis. If functional group substitution leads to an associative interaction, this self-assembly between individual polymer networks could allow for the creation of strong binding sites that occur between independent networks. This approach has a number of significant advantages. In addition to removing the rigorous requirement

for substitution at both *ortho* positions across the same biphenyl bond, the spatial relationship of cooperative functional groups could be finer tuned by adjusting network packing. As a practical advantage, this strategy also allows high-performance materials to be generated without recourse to using expensive and air-sensitive Ni(cod)₂, as in typical Yamamoto polymerization⁵⁰ conditions (*vide infra*).⁵¹

The syntheses of PAF materials fulfilling these properties are presented in Scheme 2. Monomer synthesis begins with 2,5-

Scheme 2. Synthesis of Terephthalic Ester Monomers, Polymerization, And Deprotection to Yield Acidic Porous Networks^a



^aConditions: (a) (COCl)₂, PhH; ROH, pyridine, CH₂Cl₂, 79–89%. (b) Pd(dppf)Cl₂, B₂pin₂, KOAc, 1,4-dioxane, 61–67%. (c) 9 or 10, 11, cat. 12, K₂CO₃, THF/H₂O, 84–86%. (d) KOH, DMSO, 81–86%.

dibromoterephthalic acid (6), which is commercially available or easily generated from inexpensive 1,4-dibromo-2,5-dimethylbenzene.⁵² Esterification with methanol (7) or 1-nonanol (8) and Miyaura borylation⁵³ delivers functional cross-coupling partners 9 and 10. Suzuki polymerization with the same monomer used in PAF-1 synthesis (11) is enabled by Buchwald's recently disclosed palladacycle precatalyst 12,⁵⁴ delivering insoluble materials at acceptably low catalyst loadings (0.7–1.1 mol % relative to new carbon–carbon bonds). Less reactive catalysts that have been successful in the synthesis of other PAFs (e.g., Pd(PPh₃)₄)^{55,56} were ineffective in this challenging case. Nitrogen adsorption data obtained for the acidic polymers, and their ester precursors, are shown in Figure 7. The polymer derived from methyl terephthalic ester 9, [(C₆H₄-*p*-C₆H₂(CO₂CH₃)₂-C₆H₄)₂(C)] (BPP-4), presented a BET surface area of 665 m²/g. Saponification under extremely vigorous conditions (KOH, anhydrous DMSO, 150 °C), and

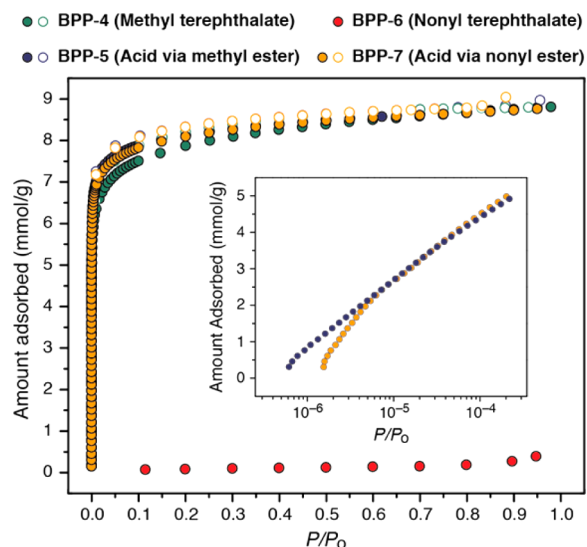


Figure 7. Low-temperature nitrogen adsorption characteristics of terphenyl-linked porous organic polymers (77 K). BPP-4: green circles, BPP-5: blue circles, BPP-6: red circles, BPP-7: yellow circles. Open circles represent desorption data.

subsequent reacidification with 3 N HCl, delivered the desired Brønsted acidic adsorbent [(C₆H₄-*p*-C₆H₂(CO₂H)₂-C₆H₄)₂(C)] (BPP-5) with a slightly increased BET surface area of 700 m²/g. Similar polymerization with 1-nonyl terephthalate ester 10 produced the nonporous polymer [(C₆H₄-*p*-C₆H₂(CO₂n-C₉H₁₉)₂-C₆H₄)₂(C)] (BPP-6). However, after side chain cleavage, the resulting acidic material, [(C₆H₄-*p*-C₆H₂(CO₂H)₂-C₆H₄)₂(C)] (BPP-7), displayed porosity effectively identical to the acidic polymer derived from 9 (705 m²/g BPP-7 vs 700 m²/g BPP-5). Again, two crucial features suggested that these frameworks were highly interpenetrated.⁵⁷ Residual bromine was below the limit of detection by EDX spectroscopy, suggesting an efficient polymerization to form terphenyl bridges. Most importantly, whereas a noninterpenetrated structure would be expected to possess a pore size on the order of 2 nm, the dominant pore size observed in methyl ester-derived acidic polymer BPP-5 is near the lower limit of N₂ detection, at ~5.4–5.6 Å (Figure 8). Interestingly, this pore size is entirely absent in the 1-nonyl ester-derived material BPP-7, likely the result of the larger 1-nonanol side chains preventing extremely dense network packing. A corresponding increase is seen in pore sizes ranging from ~6.0–6.5 Å.

Not only do these polymers display a high density of functional groups (up to 6.0 mmol/g for an ideal polymerization), they also function to simultaneously interrogate the hypotheses mentioned in our design plan. If the ammonia uptake demonstrated by the materials is only dependent upon gas-phase pK_a^{58–61} then the uptake at low pressure would be expected to be vastly inferior to the much more acidic PPN-6-SO₃H. However, if cooperative interactions could significantly enhance the adsorption enthalpy, the opposite could be observed. Furthermore, this would strongly suggest that a cooperative interaction between individual polymer networks is possible, given the *para* substitution in these particular materials. Additionally, if the interaction is between polymer networks, then the packing effects that are suggested by differences in pore size distribution should also affect ammonia uptake. Ammonia adsorption data for these materials are shown in Figure 9. Significant differences can be observed at both low

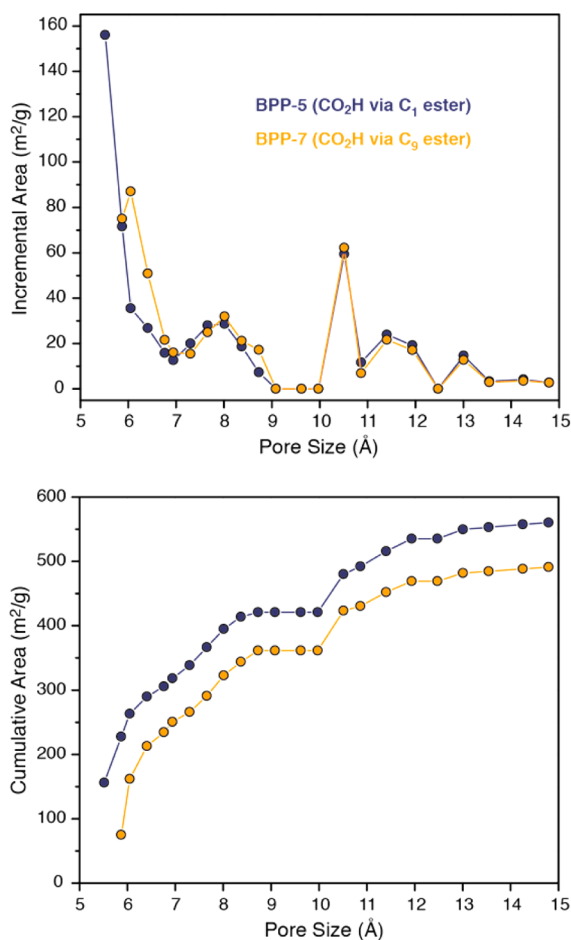


Figure 8. Effect of terephthalate ester size on pore size distribution after saponification. Methyl ester derived polymer BPP-5 = blue. 1-Nonyl ester derived polymer BPP-7 = yellow.

and high pressure. Most importantly, the carboxylic acid-substituted materials display vastly increased ammonia adsorption, especially at low pressure, where binding to the acidic functional groups takes place. Given that these results cannot be explained by gas-phase acidity (e.g., gas-phase ionization ΔG for $C_6H_5CO_2H = 1393$ kJ/mol vs $C_6H_5SO_3H < 1318$ kJ/mol).^{58–61} Additional information that can be gathered from including desorption data indicates that kinetics effects cannot be ignored in these materials. Even with extended equilibration times, BPP-5 displays lower uptake at and below 1 mbar, yet retains more ammonia at these pressures upon desorption. This strongly suggests that there is a difference in kinetics resulting from the differing pore size distributions. Very small pores—potentially, even below our limit of detection with N_2 adsorption analysis—are difficult to access, and as such, adsorption does not occur on a reasonable time scale until higher pressures are applied. At 1000 mbar, BPP-5 does display a meaningful increase over BPP-7 (17.7 mmol/g for BPP-5 vs 16.1 mmol/g for BPP-7), effectively matching Fe-MIL-101-SO₃H. Upon desorption, the higher fraction of very small pore binding sites in BPP-5 leads to greater amounts of residual adsorption (5.3 mmol/g at 203 ppm for BPP-5 vs 4.5 mmol/g at 204 ppm desorption for BPP-7).

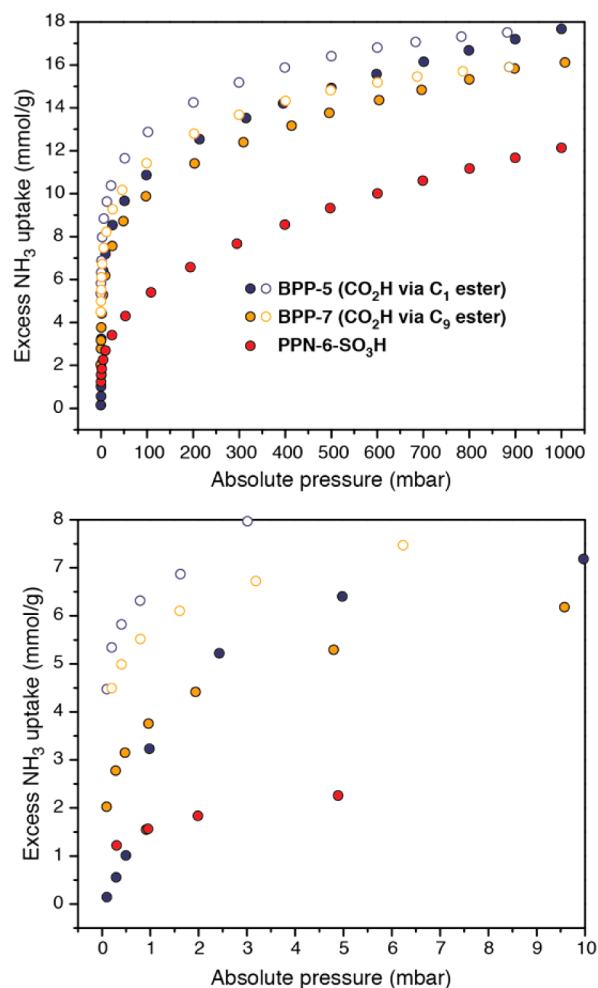


Figure 9. Comparison of room temperature (298 K) ammonia adsorption for terephthalic acid-based porous organic polymers and PPN-6-SO₃H. Carboxylic acid derived from methyl ester (BPP-5): blue circles. Carboxylic acid derived from 1-nonyl ester (BPP-7): yellow circles. Sulfonic acid (PPN-6-SO₃H): red circles. Open circles represent desorption data.

4. CONCLUSIONS

MOFs featuring highly acidic Brønsted acid sites have been developed in the context of proton conducting materials^{62–64} and heterogeneous catalysis.⁶⁵ We have shown herein that these materials can display excellent ammonia adsorption characteristics, which are competitive with more common approaches based on Lewis acidic adsorbents. Porous organic polymers based on the predictable modular assembly of rigid building blocks⁶⁶ have the potential to provide the same designed binding environments found in MOFs, while affording the exceptional chemical stability more commonly associated with traditional adsorbents such as zeolites and activated carbons, which may be required for challenging applications such as high-pressure reversible ammonia storage. The foregoing results detail a general strategy that can provide access to porous adsorbents displaying a combination of functional group density and chemical stability that rivals current champion materials. Suzuki polymerization using readily accessible precursors, along with modern catalysts showing high activity and functional group tolerance, will allow for the introduction of diverse binding sites—including those that may be difficult to incorporate in MOFs. As a specific realization of this

concept, the successful invention of a high-capacity ammonia adsorbent has been demonstrated. The superior stability of this material under extremely basic conditions suggests that multiple adsorption/desorption cycles and long-term ammonia exposure will be tolerated. Fundamental studies toward expanding the range of pore sizes available in these materials, further characterization of the proposed binding site, and additional application-driven investigations are currently underway.

■ ASSOCIATED CONTENT

● Supporting Information

Full experimental procedures, thermal gravimetric analysis, infrared, ^1H , ^{13}C , and ^{11}B NMR data, powder X-ray diffraction, EDX spectra, and elemental analyses are provided. This material is available free of charge via the Internet at <http://pubs.acs.org>.

■ AUTHOR INFORMATION

Corresponding Author

jrlong@berkeley.edu

Notes

The authors declare no competing financial interest.

■ ACKNOWLEDGMENTS

This research was supported through the Center for Gas Separations Relevant to Clean Energy Technologies, an Energy Frontier Research Center funded by the U.S. Department of Energy, Office of Science, Office of Basic Energy Sciences under award DE-SC0001015. We thank the 11-BM and 17-BM staff at the Advanced Photon Source at Argonne National Laboratory for assisting with powder X-ray diffraction experiments. Use of the Advanced Photon Source at Argonne National Laboratory was supported by the U.S. Department of Energy, Office of Science, Office of Basic Energy Sciences, under contract no. DE-AC02-06CH11357. We thank the 11-BM and 17-BM staff at the Advanced Photon Source at Argonne National Laboratory, Dr. Wendy L. Queen, and Jarad A. Mason for assisting with powder X-ray diffraction experiments. Dr. C.-N. Kuo is thanked for helpful discussions.

■ REFERENCES

- (1) Chen, B.; Xiang, S.; Qian, G. *Acc. Chem. Res.* **2010**, *43*, 1115.
- (2) Goepfert, A.; Czaun, M.; May, R. B.; Prakash, G. K. S.; Olah, G. A.; Narayanan, S. R. *J. Am. Chem. Soc.* **2011**, *133*, 20164.
- (3) McDonald, T. M.; Lee, W. R.; Mason, J. A.; Wiers, B. M.; Hong, C. S.; Long, J. R. *J. Am. Chem. Soc.* **2012**, *134*, 7056.
- (4) Didas, S. A.; Kulkarni, A. R.; Sholl, D. S.; Jones, C. W. *ChemSusChem* **2012**, *5*, 2058.
- (5) Demessence, A.; D'Alessandro, D. M.; Foo, M. L.; Long, J. R. *J. Am. Chem. Soc.* **2009**, *131*, 8784.
- (6) McDonald, T. M.; D'Alessandro, D. M.; Krishna, R.; Long, J. R. *Chem. Sci.* **2011**, *2*, 2022.
- (7) Lu, W.; Sculley, J. P.; Yuan, D.; Krishna, R.; Wei, Z.; Zhou, H.-C. *Angew. Chem., Int. Ed.* **2012**, *51*, 7480.
- (8) Das, A.; Choucair, M.; Southon, P. D.; Mason, J. A.; Zhao, M.; Kepert, C. J.; Harris, A. T.; D'Alessandro, D. M. *Microporous Mesoporous Mater.* **2013**, *174*, 74.
- (9) Danon, A.; Stair, P. C.; Weitz, E. *J. Phys. Chem. C* **2011**, *115*, 11540.
- (10) Planas, N.; Dzubak, A. L.; Poloni, R.; Lin, L.-C.; McManus, A.; McDonald, T. M.; Neaton, J. B.; Long, J. R.; Smit, B.; Gagliardi, L. *J. Am. Chem. Soc.* **2013**, *135*, 7402.
- (11) *Permissible Exposure Limits for Chemical Contaminants*; Cal/OSHA: Oakland, CA; http://www.dir.ca.gov/title8/5155stable_acl.html (accessed on October 3, 2013).
- (12) MacDonald, S. A.; Hinsberg, W. D.; Wendt, H. R.; Clecak, N. J.; Willson, C. G.; Snyder, C. D. *Chem. Mater.* **1993**, *5*, 348.
- (13) Lin, I.-K.; Bai, H.; Wu, B.-J. *Aerosol Air Qual. Res.* **2010**, *10*, 245.
- (14) Kitajima, H.; Shiramizu, Y. *IEEE Trans. Semicond. Manuf.* **1997**, *10*, 267.
- (15) Schuth, F.; Palkovits, R.; Schlogl, R.; Su, D. S. *Energ. Environ. Sci.* **2012**, *5*, 6278.
- (16) Li, J.; Chang, H.; Ma, L.; Hao, J.; Yang, R. T. *Catal. Today* **2011**, *175*, 147.
- (17) Brandenberger, S.; Kröcher, O.; Tissler, A.; Althoff, R. *Catal. Rev.* **2008**, *50*, 492.
- (18) O'Keeffe, M.; Yaghi, O. M. *Chem. Rev.* **2012**, *112*, 675.
- (19) Getman, R. B.; Bae, Y.-S.; Wilmer, C. E.; Snurr, R. Q. *Chem. Rev.* **2012**, *112*, 703.
- (20) Sumida, K.; Rogow, D. L.; Mason, J. A.; McDonald, T. M.; Bloch, E. D.; Herm, Z. R.; Bae, T.-H.; Long, J. R. *Chem. Rev.* **2012**, *112*, 724.
- (21) Suh, M. P.; Park, H. J.; Prasad, T. K.; Lim, D.-W. *Chem. Rev.* **2012**, *112*, 782.
- (22) Li, J.-R.; Sculley, J.; Zhou, H.-C. *Chem. Rev.* **2012**, *112*, 869.
- (23) Wang, C.; Xie, Z.; de Krafft, K. E.; Lin, W. *J. Am. Chem. Soc.* **2011**, *133*, 13445.
- (24) Yanai, N.; Kitayama, K.; Hijikata, Y.; Sato, H.; Matsuda, R.; Kubota, Y.; Takata, M.; Mizuno, M.; Uemura, T.; Kitagawa, S. *Nat. Mater.* **2011**, *10*, 787.
- (25) Glover, T. G.; Peterson, G. W.; Schindler, B. J.; Britt, D.; Yaghi, O. *Chem. Eng. Sci.* **2011**, *66*, 163.
- (26) Doonan, C. J.; Tranchemontagne, D. J.; Glover, T. G.; Hunt, J. R.; Yaghi, O. M. *Nat. Chem.* **2010**, *2*, 235.
- (27) Furukawa, H.; Ko, N.; Go, Y. B.; Aratani, N.; Choi, S. B.; Choi, E.; Yazaydin, A. Ö.; Snurr, R. Q.; O'Keeffe, M.; Kim, J.; Yaghi, O. M. *Science* **2010**, *329*, 424.
- (28) Spanopoulos, I.; Xydias, P.; Malliakas, C. D.; Trikalitis, P. N. *Inorg. Chem.* **2013**, *52*, 855.
- (29) Saha, D.; Deng, S. *J. Colloid Interface Sci.* **2010**, *348*, 615.
- (30) Petit, C.; Bandosz, T. J. *Adv. Funct. Mater.* **2010**, *20*, 111.
- (31) Cavka, J. H.; Jakobsen, S. r.; Olsbye, U.; Guillou, N.; Lamberti, C.; Bordiga, S.; Lillerud, K. P. *J. Am. Chem. Soc.* **2008**, *130*, 13850.
- (32) Morris, W.; Doonan, C. J.; Yaghi, O. M. *Inorg. Chem.* **2011**, *50*, 6853.
- (33) Rose, M.; Bohlmann, W.; Sabo, M.; Kaskel, S. *Chem. Commun.* **2008**, 2462.
- (34) Ben, T.; Ren, H.; Ma, S.; Cao, D.; Lan, J.; Jing, X.; Wang, W.; Xu, J.; Deng, F.; Simmons, J. M.; Qiu, S.; Zhu, G. *Angew. Chem., Int. Ed.* **2009**, *48*, 9457.
- (35) Stockel, E.; Wu, X.; Trewin, A.; Wood, C. D.; Clowes, R.; Campbell, N. L.; Jones, J. T. A.; Khimiyak, Y. Z.; Adams, D. J.; Cooper, A. I. *Chem. Commun.* **2009**, 212.
- (36) Weston, M. H.; Peterson, G. W.; Browe, M. A.; Jones, P.; Farha, O. K.; Hupp, J. T.; Nguyen, S. T. *Chem. Commun.* **2013**, *49*, 2995.
- (37) Peterson, G.; Farha, O.; Schindler, B.; Jones, P.; Mahle, J.; Hupp, J. *J. Porous Mater.* **2012**, *19*, 261.
- (38) Lu, W.; Yuan, D.; Sculley, J.; Zhao, D.; Krishna, R.; Zhou, H.-C. *J. Am. Chem. Soc.* **2011**, *133*, 18126.
- (39) Trofimov, B. A. *Sulfur Reports* **1992**, *11*, 207.
- (40) Merino, E.; Verde-Sesto, E.; Maya, E. M.; Iglesias, M.; Sánchez, F.; Corma, A. *Chem. Mater.* **2013**, *25*, 981.
- (41) Akiyama, G.; Matsuda, R.; Sato, H.; Takata, M.; Kitagawa, S. *Adv. Mater.* **2011**, *23*, 3294.
- (42) Menke, J. B. *Recl. Trav. Chim. Pays-Bas* **1925**, *44*, 141.
- (43) Helminen, J.; Paatero, E.; Turunen, I. *J. Chem. Eng. Data* **2001**, *46*, 391.
- (44) Petit, C.; Bandosz, T. J. *J. Phys. Chem. C* **2009**, *113*, 3800.
- (45) Petit, C.; Kante, K.; Bandosz, T. J. *Carbon* **2010**, *48*, 654.
- (46) Petit, C.; Bandosz, T. J. *Microporous Mesoporous Mater.* **2008**, *114*, 137.

- (47) Yu, D.; Ghosh, P.; Snurr, R. Q. *Dalton Trans.* **2012**, *41*, 3962.
- (48) Ermer, O. *J. Am. Chem. Soc.* **1988**, *110*, 3747.
- (49) Zhang, Y.-B.; Su, J.; Furakawa, H.; Yun, Y.; Gándara, F.; Duong, A.; Zou, X.; Yaghi, O. M. *J. Am. Chem. Soc.* **2013**, *135*, 16336.
- (50) Kanbara, T.; Saito, N.; Yamamoto, T.; Kubota, K. *Macromolecules* **1991**, *24*, 5883.
- (51) Palladium-catalyzed cross coupling has been used successfully to produce terphenyl-linked PAFs that do not have functional groups: Rose, M.; Klein, N.; Bohlmann, W.; Bohringer, B.; Fichtner, S.; Kaskel, S. *Soft Matter* **2010**, *6*, 3918.
- (52) Yao, Y.; Tour, J. M. *Macromolecules* **1999**, *32*, 2455.
- (53) Ishiyama, T.; Murata, M.; Miyaura, N. *J. Org. Chem.* **1995**, *60*, 7508.
- (54) Kinzel, T.; Zhang, Y.; Buchwald, S. L. *J. Am. Chem. Soc.* **2010**, *132*, 14073.
- (55) Jing, X.; Sun, F.; Ren, H.; Tian, Y.; Guo, M.; Li, L.; Zhu, G. *Microporous Mesoporous Mater.* **2013**, *165*, 92.
- (56) Zhang, K.; Kopetzki, D.; Seeberger, P. H.; Antonietti, M.; Vilela, F. *Angew. Chem., Int. Ed.* **2013**, *52*, 1432.
- (57) The illustration in Scheme 2 is meant to illustrate multifold interpenetration (>2×), rather than precise and uniform 3-fold interpenetration.
- (58) McMahon, T. B.; Kebarle, P. *J. Am. Chem. Soc.* **1977**, *99*, 2222.
- (59) Koppel, I. A.; Taft, R. W.; Anvia, F.; Zhu, S.-Z.; Hu, L.-Q.; Sung, K.-S.; DesMarteau, D. D.; Yagupolskii, L. M.; Yagupolskii, Y. L. *J. Am. Chem. Soc.* **1994**, *116*, 3047.
- (60) Smith, J. D.; O'Hair, R. A. J.; Williams, T. D. *Phosphorus, Sulfur Silicon Relat. Elem.* **1996**, *119*, 49.
- (61) Taft, R. W.; Bordwell, F. G. *Acc. Chem. Res.* **1988**, *21*, 463.
- (62) Sadakiyo, M.; Yamada, T.; Kitagawa, H. *J. Am. Chem. Soc.* **2009**, *131*, 9906.
- (63) Hurd, J. A.; Vaidhyanathan, R.; Thangadurai, V.; Ratcliffe, C. I.; Moudrakovski, I. L.; Shimizu, G. K. H. *Nat. Chem.* **2009**, *1*, 705.
- (64) Yoon, M.; Suh, K.; Natarajan, S.; Kim, K. *Angew. Chem., Int. Ed.* **2013**, *52*, 2668.
- (65) Lee, J.; Farha, O. K.; Roberts, J.; Scheidt, K. A.; Nguyen, S. T.; Hupp, J. T. *Chem. Soc. Rev.* **2009**, *38*, 1450.
- (66) Zou, X.; Ren, H.; Zhu, G. *Chem. Commun.* **2013**, *49*, 3911.